The centrosome-nucleus complex and microtubule organization in the Drosophila oocyte.

Jens Januschke, Louis Gervais, Laurent Gillet, Guy Keryer, Michel Bornens, Antoine Guichet

This is an author-prepared version of a manuscript published in Development vol 133 pp 129-139 doi:10.1242/dev.02179

The Centrosome-Nucleus complex and microtubule organization in the *Drosophila* oocyte

Jens Januschke[1*], Louis Gervais[1*], Laurent Gillet[1], Guy Keryer[2], Michel Bornens[2], Antoine Guichet[1]

[1]Institut Jacques Monod, Unité Mixte Recherche 7592, CNRS, Université Paris 6 et Paris 7, 2 place Jussieu, F-75251, Paris Cedex 05, France.

[2]Institut Curie, Section Recherche, Unité Mixte Recherche 144, CNRS, 75248Paris, France.

* These authors contributed equally to this work

Author for correspondence:

Antoine Guichet

guichet@ijm.jussieu.fr

Tel: 00 33 1 44 27 40 94

fax: 00 33 1 44 27 52 65

(7093 words)

ABSTRACT

Molecular motors transport the axis-determining mRNAs *oskar*, *bicoid* and *gurken* along microtubules (MTs) in the *Drosophila* oocyte. However, it remains unclear how the underlying MT network is organized and how this transport takes place. We have identified a centriole-containing centrosome close to the oocyte nucleus. Remarkably, the centrosomal components, γ-tubulin and *Drosophila* pericentrin-like protein also strongly accumulate at the periphery of this nucleus. MT polymerization after cold-induced disassembly in wild-type and in *gurken* mutants suggests that in the oocyte, the centrosome-nucleus complex is an active centre of MT polymerization. We further report that the MT network comprises two perpendicular MT subsets that undergo dynamic rearrangements during oogenesis. This MT reorganization parallels the successive steps in localization of *gurken* and *oskar* mRNAs.

We propose that in addition to a highly polarized microtubule scaffold specified by the cortex oocyte, the repositioning of the nucleus and its tightly associated centrosome could control MT reorganization and hence, oocyte polarization.

INTRODUCTION

The MT cytoskeleton of eukaryotic cells is involved in many cellular functions. MTs allow delivery of cellular components to specific intracellular locations by means of MT motors, but how MT arrays contribute to polarized transport remains a central question. The *Drosophila* oocyte provides an excellent model system to study polarized MT dependent transport since MTs control the localization of several transcripts encoding axis determinants (for review, see (Palacios and St Johnston, 2001)). The ovarian egg chamber consists of a cluster of 16 interconnected germ cells, surrounded by a monolayer of follicular epithelium. During egg chamber formation, one cell of the cluster is singled out to become the oocyte while its 15 sister cells develop into nurse cells. This process of oocyte specification requires polar transport of oocyte determinants mediated by minus-end directed MT motors (for review, see (Palacios and St Johnston, 2001)). MT nucleation is believed to be restricted to the posterior of the oocyte from where MTs extend through the ring canals into the nurse cells. The MT organization in the oocyte is unchanged until mid-oogenesis at the onset of stage 7. Then, a signal emitted from the overlaying follicle cells triggers the reorganization of the MT network and the migration of the nucleus to the anterior. Subsequently, *bicoid* (*bcd*) mRNA, is localized to the anterior cortex of the oocyte. *oskar* (*osk*) mRNA, is transported to the posterior pole and *gurken* (*grk*) mRNA, is localized to an antero-dorsal cap near the oocyte nucleus (reviewed in (Riechmann and Ephrussi, 2001)). The localization of these axes determining transcripts occurs in several steps and is dependent on MTs, cytoplasmic Dynein and Kinesin I. During the period critical for mRNA localization (stage 7-9), MTs are distributed in an antero-posterior gradient, the highest concentration occurring in the anterior part of the oocyte (Theurkauf et al., 1993; Theurkauf et al., 1992; Clark et al., 1997; Micklem et al., 1997). The orientation of MTs within this gradient was determined using minus and plus end markers, i.e. Nod-βgal and Kinesin-βgal, respectively (Clark et al., 1994; Clark et

al., 1997). However, the use of these markers was not sufficient to explain the successive MT dependent localization steps of *osk* and *grk* mRNA. Furthermore, the behavior of the MTOC during oogenesis is complex and the localization and nature of the MTOC during this period are unknown. Shortly after oocyte specification, nurse cell centrosomes migrate toward the oocyte where they eventually accumulate at the posterior of the nucleus (Bolivar et al., 2001; Mahowald and Strassheim, 1970). Centrioles reportedly disappear since they could not be detected after stage 4 (Mahowald and Strassheim, 1970), whereas the PCM is still associated with the oocyte nucleus where γ-tubulin, Centrosomin and Pericentrin/AKAP450 can be easily detected (Martinez-Campos et al., 2004; Tavosanis and Gonzalez, 2003). From stage 1 to stage 6, MTs are nucleated from a posterior MTOC and at the end of stage 9, PCM components belonging to the γ–TuRC complex have been found at the anterior and lateral cortices (Cha et al., 2002; Schnorrer et al., 2002). However, during the stages 7 to 8, the nature of the MTOC remains elusive.

In the present work we have studied the nucleation and the organization of the MT network in the oocyte in order to better understand mRNA transport. We show that the association of a centriole-containing centrosome with the nucleus surrounded by PCM material constitutes a MTOC. Using a new fixation method that allows detection of essential components of the MT network and MTOC, we found that the oocyte contains two different MT populations. The two MT populations evolve differentially during oogenesis, which could constitute a scaffold for differential mRNA transport.

RESULTS

A centrosome localizes close to the oocyte nucleus during mid-oogenesis

Both the nature and the localization of the MTOC beyond stage 6 of *Drosophila* oogenesis have not yet been clarified. Up to stage 6, γ-tubulin has been shown to closely associate with

the nucleus at the posterior of the oocyte. In addition, electron microscopy studies have demonstrated the presence of centrioles close to the oocyte nucleus up to stage 4 (Mahowald and Strassheim, 1970). Thus, until stage 6, the centrosome associates with the nucleus at the posterior of the oocyte. In *Drosophila* females, meiosis takes place in the absence of centrosomes (Mahowald and Strassheim, 1970). It has therefore been speculated that, at stage 6, centrosome organization changes, involving the disappearance of centrioles and the generation of MTs from a diffuse organizing centre. To better understand this process, we re-investigated the distribution of γ–tubulin in the oocyte. Before re-polarization of the MT cytoskeleton, we found that γTub23C and γTub37C (Sampaio et al., 2001; Sunkel et al., 1995) localize in a layer around the nucleus, with an enrichment at the posterior pole of the oocyte (Fig. 1 A). This is in agreement with the location of the MTOC at this stage. After re-polarization of the MT cytoskeleton, both γ–tubulin isoforms remain located in a perinuclear manner (Fig. 1, B and C). Interestingly, γTub37C, but not γTub23C, labels a small body close to the oocyte nucleus (Fig. 1, compare A to C). In addition, γTub37C and γTub23C also exhibit differential expression patterns in embryos: γTub37C is located with the centrosomes of mitotic cells, whereas γTub23C is not (Tavosanis and Gonzalez, 2003). Thus, γ–tubulin is distributed in close association with the nucleus periphery and possibly on a centrosome-like structure. Pericentrin/AKAP450 is another major component of the centrosome. Green fluorescent protein (GFP) fusion of the C-terminal part of Pericentrin/AKAP450 and its *Drosophila* homologue pericentrin-like protein (D-PLP) have been shown to localize to the centrosomes respectively in cultured human cells (Keryer et al., 2003), *Drosophila* embryos and spermatocytes (Martinez-Campos et al., 2004; Rebollo et al., 2004). Using the UAS/Gal4 system (Brand and Perrimon, 1993) we specifically expressed GFP-cter-D-PLP, in the germ line and detected a bright dot in the vicinity of the nucleus before and after nuclear migration (Fig. 1 D). GFP-cter-D-PLP is also detected in all germ line nuclei as has been observed

previously (Martinez-Campos et al., 2004). From stage 7 onwards, the bright dot remained in the immediate vicinity of the oocyte nucleus (<1 µm distance, Table I). Furthermore, both GFP-cter-D-PLP and γTub37C colocalize to this discrete body, indicating that this structure could correspond to a centrosome (Fig. 1, E-G). In G2 centriole tubulin is highly polyglutamilated (Bobinnec et al., 1998). The ID5 antibody labels basal bodies and centrioles in several species (Beisson et al., 2001). Using this antibody, we detected a dot close to the nucleus throughout oogenesis that remains detectable up to stage 10A (Fig. 1 H). This suggests that the dot represents a centriole-containing centrosome. Indeed, using electron microscopy, (Fig. 1 I, J), we clearly detected 2 to possibly 4 centrioles closely associated with the nucleus in stage 9 oocytes. This demonstrates the existence of centrioles associated with the nucleus at least up to stage 9. We could not unambiguously detect MT fibers emanating from those centrioles. We then analyzed the link between centrosome and nucleus using colchicine. In flies fed with colchicine, MTs in the germ line are completely de-polymerized and the oocyte nucleus is mispositioned (Fig. 1 L). In the oocyte, we observed that the nucleus and the centrosome are significantly separated, the distance between them increasing during oocyte growth (Fig. 1 M, N and Table I.). In a few cases, we noticed that the nucleus can reach the anterior cortex without the centrosome; however, we never observed a centrosome at the anterior without the nucleus (Table 1). We conclude that the close localization of the centriole-containing centrosome to the nucleus depends on MTs.

Two differently orientated MT subsets are present in the oocyte

The structure of the MT network during mid-oogenesis is dynamic. At stage 7, MTs are visible as a mesh at the anterior cortex. Later, at stage 10, MT bundles are observed that promote cytoplasmic streaming (Theurkauf et al., 1993; Theurkauf et al., 1992).

In-between MT distribution has been described as an antero-posterior gradient (Micklem et al., 1997) However, high resolution images of oocyte MTs are lacking. Therefore, we modified for the *Drosophila* egg chamber a protocol frequently used to increase the detection of the MT cytoskeleton in cell culture to characterize MT organization in the oocyte during the critical period in which *bcd*, *grk* and *osk* mRNAs are localized. We detected MTs throughout oogenesis using αTubulin but also with a Kinesin heavy chain antibody (α-Khc), which reveal the MT array and its complexity in unprecedented definition (Fig. 2, A-B). We noticed that the range of detected details was increased and more reproducible with α-Khc antibody. To control the specificity of Khc detection, we generated germ line and follicle cells mutant clones homozygous for $khc^{7.288}$. In such mutant cells, no Khc is detected (Fig. 2, B inset), indicating that the detection is specific. Labelling with antibodies directed against aromatic c-terminal amino acid residues (Tyr or Phe) of α-tubulin (Badin-Larcon et al. 2004**)** and against Khc largely overlaps (Fig. 2 I, J). This confirmed that the structures revealed by Khc are MTs. We also detected a Khc fraction at the posterior of the oocyte (Fig. 2 J) as it has been previously shown (Brendza et al. 2002). That Khc accumulates along MTs may be due to permeabilization prior to fixation, which could cause rigor binding of Khc to MTs. Such case has been observed for the motor XKCM1 without affecting MT organization itself (Walczak et al., 1996). This detection procedure may also permit the extraction of a soluble pool of Khc and reveal the remaining fraction distributed along the MTs (Hollenbeck, 1989). With our detection procedure, Khc revealed by Kinesin-βgal (Clark et al., 1994) exhibits a more restricted distribution compared to α-Khc antibody (Fig. 3H, I). This is likely due to the substitution of the c-terminal part of Khc by the β-galactosidase in the reporter construct, impairing the recycling of the chimeric Kinesin motor leading to its accumulation exclusively at the posterior. We also show that with our detection method, the MT minus end marker, Nod-βgal, is detected to the antero dorsal corner above the oocyte nucleus as well as to the

opposite antero ventral corner (Fig. 3J, K) as it has been reported before (Clark et al., 1997; MacDougall et al., 2003). Moreover, localized determinants like Osk and Grk are correctly positioned in the oocyte (Fig. 3L, M).

To confirm that our detection method does not alter MT organization, we analyzed MT distribution in follicle cells, which should be sensitive to the extraction procedure as they are more directly exposed than the oocyte (Fig. 3 A-E). MT distribution in different follicle cell types was unchanged, when comparing living and fixed egg chambers. The main body follicle cell MTs seemed unchanged (Fig.3 D, E). Main body follicle cell MTs have been shown to be highly stable, and might therefore reflect the sensitivity of the protocol with limitations (Doerflinger et al. 2003). Nevertheless, stretched follicle cells showed strikingly similar MT patterns in living and fixed conditions as well (Fig.3 B, C). Apical-basal polarity was not affected in follicle cells, as demonstrated by the correct apical localization of atypical protein kinase C (Fig. 3 F, G). Importantly, the MT distribution, of living egg chambers expressing GFP- αTubulin at stage 7 (Fig. 2 C) and stage 9 (Fig. 2 F) is similar to the one observed using anti αTubulin and Khc antibodies. (Fig. 2 D, E, G, H). Therefore it seems that our fixation conditions preserve the wild-type MT organization and that Khc can be suitable to label bulk MTs.

When fixed WT oocytes were analyzed by confocal microscopy, MT organization in the oocyte appeared unchanged from stage 2 (data not shown) to stage 6 (Fig. 4 B, 1-5). With stage 7 (~60% *n*=11), MT organization was modified and two MT subsets became apparent. This organization was more evident at stage 8 (~69% *n*=23). A first subset consists of cortical MTs oriented along the dorso-ventral (DV) axis parallel to the oocyte nurse cell border, and juxtaposed to the lateral cortices, wrapping the oocyte from stage 7 to 9 (Fig. 4 C – E, 1 and 5). At least some MT bundles of this subset can be traced back to the oocyte nucleus. The DV

orientation of MT bundles, depicted as black fibers in the schematic representations (Fig. 4 C 6; D 6; E 6), is highly reproducible for all stages and persists throughout mid-oogenesis.

A second MT subset, depicted as red fibers in the schematic representations (Fig. 4 C 6; D 6; E 6), is present in the centre of the oocyte. Although there was some variability in the patterns observed, we found that each developmental stage showed a characteristic MT distribution. During stage 6 (~82% *n*=17), MTs from this subset are cortical and extend from the nucleus at the posterior to the anterior cortex (Fig. 4 B, 2-4). At stage 7 (~90% *n*=11), compact bundles of MTs form a circle-like structure resembling a diaphragm. This subset is formed by long MT bundles that extend (once or more) along the entire cortex (Fig. 4 C, 2-4). By stage 8 (~65% *n*=23), the oocyte has considerably grown and individual MT bundles are therefore easier to track. MT bundles emanate from the anterior and the nucleus to point toward the posterior (Fig. 4 D, 2). MTs extend again along the entire cortex after which they turn to the central cytoplasm (Fig. 3 D, 3). This, in turn, generates free MT (plus) ends in the centre of the oocyte (Fig. 4 D 4). By stage 9 (~72% *n*=18), the central MT network is clearly oriented along the oocyte AP axis. One or two thick MT bundles extend from the anterior, pointing toward the posterior pole. These bundles form a structure resembling a horse shoe with its open side facing the posterior (Fig. 4 E, 2 - 4). Importantly, both subsets could also be detected in living egg chambers as shown for the DV subset (Fig. 4 F, H) and the AP subset (Fig. 4 G). Thus, MTs show strong rearrangements throughout mid-oogenesis which result in two perpendicular MT arrays reflecting the two axes of the oocyte.

The centrosome-nucleus complex is an active centre for MT nucleation in the oocyte

We developed an ex vivo assay to localize MT nucleation sites by dissecting ovaries and placing them on ice for 30 min. This treatment results in complete de-polymerization of MTs (Fig. 5 B). When allowed to recover at 25°C for 30min, MT distribution could be re-

established to the WT situation, where both the cortical and the central subsets of MTs were detectable (Fig. 5 I, J). γ-tubulin distribution was not affected by cold-induced MT de-polymerization (Fig. 5 C). When short periods of regrowth were analyzed, MT nucleation appeared limited to the close vicinity of the nucleus and was often asymmetric (Fig. 5 D, E), suggesting a centrosome associated nucleation activity. MT regrowth appeared to be stepwise, as after 15 min, only the DV cortical subset was established. MTs clustered around the oocyte nucleus and aligned along the cortex in DV direction (Fig. 5 F, G). The cortical location of these fibers was clearly revealed by the presence of Khc positive dots at either the dorsal or the ventral side (Fig. 5 H). This indicates that the DV MT subset is the first to regrow. We repeated the regrowth experiment using colchicine. After the drug was washed out, MT re-polymerization was observed at the oocyte nucleus (data not shown). Taken together, these results indicate that at least with our detection method, the oocyte nucleus and its immediate surrounding have the capacity to nucleate MTs.

The MT network is inverted in *grk* mutants

To test whether the centrosome-nucleus complex could direct the re-polarization of the MT network, we analyzed how MTs distribute in *grk* mutant oocytes. In this mutant, the nucleus frequently remains at the posterior of the oocyte due to a failure in the signalling cascade that induces the re-polarization of the cytoskeleton (Gonzalez-Reyes et al., 1995; Roth et al., 1995). In *grk* mutant oocytes similar in size to WT stage 8, the MT distribution was dramatically affected. Specifically, we found that MT organization appeared completely reversed compared to WT, where the nucleus is at the anterior and MT plus-ends are located

toward the posterior at stage 8 (Fig. 6 A, B vs. Fig. 6 E, F). In slightly older oocytes, MTs remain stretched out along the cortex from the posterior toward the anterior where they fold back to the centre of the oocyte (Fig. 6 B). MT ends in the centre are most likely plus ends since the pool of Khc (localized at the posterior of WT oocytes, Fig. 3 I) colocalizes with Kinesin-βGal to the centre of the oocyte, between the flanking MT ends (Fig. 6 D, G (Clark et al., 1994)). Interestingly, MT distribution in *grk* oocytes was strikingly similar to MTs of WT egg chambers prior to the migration of the oocyte nucleus (Fig. 6, E and F). Likewise, the centrosome, as revealed by γ-tubulin, which is found at the posterior of stage 6 WT oocytes, stays at the posterior in *grk* mutants (Fig. 6 H). Thus, in *grk* mutants, distribution of MT and MTOC seemed similar to their distribution in WT stage 6.

grk mutant oocytes having mispositioned nuclei provide an ideal basis to test the MT nucleating capacity of the centrosome-nucleus complex using the cold-shock assay. After cold-shock treatment of *grk* oocytes, we checked for complete MT de-polymerization (Fig, 6 I). As in the WT, during the initial period of recovery at 25°C, MT polymerization took only place in the immediate vicinity of the mispositioned oocyte nucleus (Fig. 6 J). Therefore, as in WT oocytes, MT nucleation is often asymmetric and restricted to the area surrounding the nucleus. This result strengthens the possibility that the centrosome-nucleus complex is an active MTOC.

DISCUSSION

In polarized cells, the MT network is oriented to allow the delivery of cellular components to specific locations. Here we show that in the *Drosophila* oocyte, a centriole-containing centrosome is present in close association with the nucleus, which itself is covered by PCM components until late in oogenesis. In addition, we show that MTs can nucleate from this centrosome-nucleus complex. The MTs appear to form two orthogonal MT populations that

develop through several steps during mid-oogenesis. We propose that the migration of the nucleus in the oocyte could control the reorganization of the MT network.

The centrosome and the nucleus could constitute a Microtubule Organizing Centre in the oocyte

In region 2 of the germarium, nurse cell centrosomes migrate toward the oocyte. Later, in region 3, these centriole-containing centrosomes become located as an aggregate between the oocyte nucleus and the follicle cell border (Mahowald and Strassheim, 1970; Bolivar et al., 2001). Pericentriolar material closely associated with the oocyte nucleus could be clearly detected until stage 6 with several centrosomal markers, such as γ-tubulin, Centrosomin and D-Tacc (Martinez-Campos et al., 2004; Tavosanis and Gonzalez, 2003). From stage 4 onwards, the fate of the centriole cluster had been unknown (Mahowald and Strassheim, 1970). In this study, we show that both γTub37C and γTub23C are localized in a perinuclear manner throughout oogenesis. γTub37C highlights a discrete body close to the nucleus. This body is similarly detected by the centrosomal marker D-PLP and by a specific antibody for polyglutamylated Tubulin, which detects centrioles. Consistent with this, we have detected 2 to possibly 4 centrioles in the immediate vicinity of the nucleus in stage 9 oocytes. This result demonstrates that at least until stage 9, a centriole-containing centrosome is present in the oocyte. Currently, we do not know whether they are still present at the onset of meiosis I during stage 13 since it has previously been proposed that the meiotic spindle is achieved without centrosomes (Mahowald and Strassheim, 1970). During skeletal muscle morphogenesis, myotube centrosomes dissociate from their nuclei, centrioles disappear and the centrosomal matrix is redistributed to the nucleus periphery (Tassin et al., 1985). Similarly, during oogenesis, centrioles from nurse cell centrosomes may disappear. On the other hand, their pericentriolar material may relocate to the oocyte nucleus periphery. This

would explain the specific enrichment of the oocyte nucleus with perinuclear MTOC material. The only centrosome remaining associated with a nucleus is that of the oocyte. Furthermore, the structure of this centrosome remains intact. We conclude that the four centrioles found close to the nucleus in stage 9 may correspond to the initial oocyte centrosome in the duplication phase observed in G2.

Previous studies have shown that in the oocyte, MTs were more abundant at the anterior than at the posterior (Micklem et al., 1997; Theurkauf et al., 1993; Theurkauf et al., 1992) and that MT minus-ends are associated with the cortex (Cha et al., 2002), suggesting that MTs could be nucleated there. With this work, we did not detected MT nucleation at the lateral cortex and MT disassembly and regrowth experiments suggest that MT nucleating activity is associated with the centrosome-nucleus complex. A lack of sensitivity in our MT detection method is unlikely to explain the absence of nucleation from the oocyte cortex, since cortical MTs could be detected in fixed egg chambers. Still, we cannot exclude that our experimental procedures favour the regrowth from the oocyte nucleus. However, only some MTs can be traced back to the nucleus surrounding (supplementary material Mov1) other only to the cortex. In addition, the MT minus end marker Nod-βgal is detected at both corners of the anterior cortex. Therefore we propose that MTs are nucleated at the centrosome-nucleus complex, but only part of them is attached there, the remaining MTs might be released. Such MTs would be subsequently translocated and captured at cortical sites. MTs translocation could involve actin filaments and motor proteins. Interestingly, MT organisation in the oocyte is affected when actin organisation in impaired (Manseau et al. 1996). Such mechanism has been observed in different cell types (see for review (Bornens, 2002)). Hence, while MT nucleation is likely to be restricted to the centrosome-nucleus complex, MT minus ends are not. This would be in accordance with the observation that injected *bcd* mRNA in the oocyte accumulates at lateral cortices (Cha et al. 2001).

We have observed that MT reorganization in the oocyte after stage 6 occurs always at the onset of anterior migration of the nucleus, suggesting an association between the nucleus and the MTOC. In agreement with this, a mutation impairing the anchoring of the nucleus at the anterior cortex induced a change in the MT network (Guichet et al, 2001). Likewise, in *grk* mutant oocytes with the nucleus at the posterior, the MT network seems organized as in WT stage 6 prior to MT reorganization. MT disassembly and regrowth suggest at least with our detection method, that a MT nucleating activity is associated with the centrosome-nucleus complex both, in WT and in *grk* mutant oocytes. Interestingly, laser ablation of the nucleus at the anterior of the oocyte inhibited localization of determinants to the posterior, revealing a failure of MT-dependent posterior transport in the absence of the nucleus (Montell et al., 1991). These results are in support of a role for the centrosome-nucleus complex in the nucleation of the MT network necessary for correct polarized transport in the oocyte. Interestingly, MT nucleation from the nuclear envelope, as well as from centrosomes has been described recently in *Drosophila* spermatocytes (Rebollo et al., 2004).

Some MTOC components have been detected along the lateral cortex (Cha et al., 2002; Schnorrer et al., 2002), however, their MT nucleating activity has not been established. MT regrowth experiments under our experiment condition, argue against such lateral MTOC activity. MT nucleation activity of cortical MTOC components could be repressed, for example by a Ran GTP gradient controlled by the nucleus. This would ensure that centrosomal or non-centrosomal MTOC activity is restricted to the vicinity of the nucleus. Such a mechanism has been reported for *Xenopus* oocytes as well as for somatic cells (Gruss et al., 2001; Keryer et al., 2003).

A complex MT scaffold participates in axis specification

We are able to follow MT organization in the oocyte in high detail: cortical MTs run in parallel to the DV axis throughout oogenesis and a subset of MTs oriented in AP direction develops progressively in the centre. Using time-lapse images of GFP-Tubulin or Tau-GFP in live oocytes we were able to reproduce similar MT organization patterns as observed with fixed samples. The presence of two orthogonal subsets has been proposed earlier (MacDougal et al., 2003) and appears to be very likely adapted to specify different compartments by facilitating differential mRNA transport (Brendza et al., 2000; Cha et al., 2002; Duncan and Warrior, 2002; Januschke et al., 2002; MacDougall et al., 2003). Indeed, there is a strong correlation between MT re-distribution and mRNA localization (Fig. 7). *grk* and *osk* mRNAs show a dynamic and stage-dependent localization pattern (Ephrussi et al., 1991; Neuman-Silberberg and Schuepbach, 1993). Both mRNAs are located at the posterior prior to nuclear migration and move toward the anterior shortly after nuclear migration and reorganization of the MT cytoskeleton. From stage 7 onwards, *grk* and *osk* mRNAs show striking differences in their localization (see cartoon Fig. 7). During stage 7, *grk* localizes along the anterior margin facing the nurse cell border. During stage 8, *grk* already is restricted to the antero-dorsal corner around the oocyte nucleus (Fig. 7). This transport step is dependent on MT motors (Duncan and Warrior, 2002; Januschke et al., 2002; MacDougall et al., 2003). The DV subset, being fully established at stage 7, is a candidate for such transport. This could further explain why *grk* mRNA localization to the anterio-dorsal cap always precedes *osk* mRNA localization to the posterior. Throughout the subsequent stages, as at least some of the *grk* message arrives from the nurse cells, the DV MT subset is likely to facilitate rapid transport towards the nucleus. Likewise, *osk* mRNA localization to the posterior seems to be coupled to the central MTs. *osk* localization occurs in a step-wise manner and is only completed during stage 9. This correlates with the progressive development of the centre MT subset toward an AP

orientation. We never observed MT fibres touching the posterior cortex. Thus, *osk* mRNA transport from the posterior most ending of MTs obtained during stage 9 might rely on other uncharacterised mechanisms.

During stage 7-9 *bcd* mRNA is transported to the oocyte, where it localizes as a ring to the anterior cortex. As it enters the oocyte, *bcd* mRNA encounters MTs organized at the anterior cortex necessary for its maintenance. In *grk* mutant oocytes, *bcd* localizes to the anterior as well as to the posterior pole. The anterior localization of *bcd* suggests the presence of MT minus ends there. We did not detect MT nucleation activity at the anterior cortex in the cold-shock experiments. Therefore, posteriorly nucleated MTs might also in *grk* mutants be translocated to and anchored at the anterior cortex. However, we can not exclude that we might have missed MT nucleation activity at the cortex due to the experimental set up.

Previous data suggest that MT distribution ranges from cortical enrichment of MTs during stage 7 (Theurkauf et al., 1992), via an intermediate step with MT plus ends in the centre (Palacios and St Johnston, 2002) toward MT bundling that promotes ooplasmic streaming late in oogenesis (Theurkauf, 1994). The presence of perpendicular MT subsets has been proposed (MacDougall et al. 2003). Thus, MT organization changes dramatically during mid-oogenesis, but stage dependent configurations have not yet been established and high resolution images of MTs were missing. Our results suggest different stage dependent MT configurations. This complex oocyte-wide network, in which two MT subsets with a different spatial organization are apparent could provide a basis for MT motors to organize differential transport.

MATERIALS & METHODS

Fly stocks

w^{118} served as WT control and parental stock to generate transgenic flies. The grk^{2B6}, grk^{HK}, grk^{DC} alleles were used for mutant analysis (Neuman-Silberberg and Schuepbach, 1993). MT extremities were detected using either Kin-LacZ or Nod-LacZ (Clark et al., 1997). Germ line clones for *Khc* were generated using $Khc^{7.288}$ *FRT G13* (Januschke et al., 2002). *tubGAl4* is described in Januschke et al., 2002. MTs in living egg chambers were analyzed using polyubiquitin-GFPS65C-alphaTub84B (Rebollo et al., 2004) and Tau-GFP (Micklem et al., 1997). The last 199 amino acids of the C-terminus of CG6735 (Kawaguchi and Zheng, 2004) were amplified by PCR and cloned into the pUASpmGFP6 vector.

MT detection

MT detection was adapted from a method developed to preserve the cytoarchitecture in cells in which antibody penetration is reduced (Pizon et al., 2002). Ovaries were incubated in BRB80 buffer (80mM PIPES pH 6.8, 1mM $MgCl_2$, 1mM EGTA), containing 1% Triton X100 (BRB-80-T) for 1h at 25°C without agitation. Then ovaries were fixed in MeOH at -20°C for 15min and rehydrated 15h at 4°C in PBS 0.1% Tween, then blocked 1h in PBS 0.1% Tween containing 2% (w/v) BSA prior to incubation with primary antibody over night.

Immunohistochemistry and *in situ* hybridization

Rabbit Anti-Khc AKIN02-A (Cytoskeleton, Denver, USA) 1:250, monoclonal anti α-tubulin (DM1A) FITC Conjugate (SIGMA) 1:250, rat Anti-tyrosinated Tubulin YL 1/2 1:200 (Kilmartin

et al., 1982), mouse anti-polyglutamylated MTs on centrosomes, ID5 (Beisson et al., 2001). Rabbit anti-γ-tubulin: R46 (γTub37C, (Raynaud-Messina et al., 2001)), 1:500 dilution, Rb1011 (γTub37C, (Tavosanis and Gonzalez, 2003)) 1:5, R77 (γTub23C, (Debec et al., 1995)) 1:500. Mouse anti-Beta-galactosidase (Promega), 1:200. Rabbit anti PKCz C20 (Santa Cruz Biotechnology, Inc.), 1:1,000. Anti-Osk and anti-Grk as described in (Januschke et al., 2002). PicoGreen (Molecular Probes) 3µl/1ml PBS 0.1%Tween for 45min following RNAse A treatment 0.4µg/ml for 1h prior to staining. *In situ* hybridization was performed using *grk* and *osk* specific probes according to (Wilkie and Davis, 2001). Images were taken on a LEICA SP2 AOBS microscope (40x 1.25NA oil) except for Fig. 2 C, D, F , Fig. 3 C, E, Fig. 4 F-H, Fig. 5 E-H that were taken on a Perkin Elmer Ultra View confocal scanner. Deconvolution was carried out using the HUYGENS 2.6 software and the QMLE algorithm with 7 iterations and 3D reconstruction using the AMIRA 2.2 software. Living oocytes were dissected in BRB buffer or M3 insect medium (Sigma). Electron microscopy protocol is available upon request.

MT disassembly and regrowth

Complete de-polymerization: ovaries were incubated 30min in BRB-80-T at 25°C for 30min then placed on ice for 30min and fixed. Complete regrowth: ovaries were incubated for 30min in BRB-80-T on ice, then incubated at 25°C for 30min and subsequently fixed. Partial regrowth: Ovaries were incubated in BRB-80-T at 25°C for 27, 25, 20 or 15min, placed on ice for 30min and then transferred to 25°C for 3, 5, 10 or 15 min, respectively, then fixed and stained for MTs. Colchicine treatment: Flies were fed for 15h with colchicine [65µg /ml] and analyzed for MTs.

Acknowledgements

We thank Sophie Lepanse for the electron microscopy analysis; Veronique Pizon for suggestions on MT detection; Tristan Piolot and Christophe Chamot for microscope assistance; Christian Brändle, Jean René Huynh, Roger Karess, Anne Schmidt and Anne Marie Tassin, for critical comments on the manuscript; J. J. was supported by a fellowship from the "Association pour la recherche sur le cancer". This work was supported by grants from Centre National de la Recherche Scientifique (CNRS), Universités Paris 6 et Paris 7, Association pour la recherche sur le cancer (Arc; subventions number 4446, 3297), ACI "Biologie du Developpement et physiologie Integrative" programme of the Ministere de la Recherche, ACI "Jeune chercheur" programme of the Ministere de la Recherche.

REFERENCES

Badin-Larcon, A. C., Boscheron, C., Soleilhac, J. M., Piel, M., Mann, C., Denarier, E., Fourest-Lieuvin, A., Lafanechere, L., Bornens, M. and Job, D. (2004). Suppression of nuclear oscillations in Saccharomyces cerevisiae expressing Glu tubulin. *Proc Natl Acad Sci U S A* **101**, 5577-82.

Beisson, J., Clerot, J. C., Fleury-Aubusson, A., Garreau de Loubresse, N., Ruiz, F. and Klotz, C. (2001). Basal body-associated nucleation center for the centrin-based cortical cytoskeletal network in Paramecium. *Protist* **152**, 339-54.

Bobinnec, Y., Moudjou, M., Fouquet, J. P., Desbruyeres, E., Edde, B. and Bornens, M. (1998). Glutamylation of centriole and cytoplasmic tubulin in proliferating non-neuronal cells. *Cell Motil Cytoskeleton* **39**, 223-32.

Bolivar, J., Huynh, J. R., Lopez-Schier, H., Gonzalez, C., St Johnston, D. and Gonzalez-Reyes, A. (2001). Centrosome migration into the Drosophila oocyte is independent of BicD and egl, and of the organisation of the microtubule cytoskeleton. *Development* **128**, 1889-97.

Bornens, M. (2002). Centrosome composition and microtubule anchoring mechanisms. *Curr Opin Cell Biol* **14**, 25-34.

Brand, A. H. and Perrimon, N. (1993). Targeted gene expression as a means of altering cell fates and generating dominant phenotypes. *Development* **118**, 401-15.

Brendza, R. P., Serbus, L. R., Duffy, J. B. and Saxton, W. M. (2000). A function for kinesin I in the posterior transport of oskar mRNA and Staufen protein. *Science* **289**, 2120-2.

Brendza, R. P., Serbus, L. R., Saxton, W. M. and Duffy, J. B. (2002). Posterior localization of dynein and dorsal-ventral axis formation depend on kinesin in Drosophila oocytes. *Curr Biol* **12**, 1541-5.
Cha, B. J., Koppetsch, B. S. and Theurkauf, W. E. (2001). In vivo analysis of Drosophila bicoid mRNA localization reveals a novel microtubule-dependent axis specification pathway. *Cell* **106**, 35-46.
Cha, B. J., Serbus, L. R., Koppetsch, B. S. and Theurkauf, W. E. (2002). Kinesin I-dependent cortical exclusion restricts pole plasm to the oocyte posterior. *Nat Cell Biol* **4**, 592-8.
Clark, I., Giniger, E., Ruohola-Baker, H., Jan, L. Y. and Jan, Y. N. (1994). Transient posterior localization of a kinesin fusion protein reflects anteroposterior polarity of the Drosophila oocyte. *Current Biology* **4**, 289-300.
Clark, I. E., Jan, L. Y. and Jan, Y. N. (1997). Reciprocal localization of Nod and kinesin fusion proteins indicates microtubule polarity in the Drosophila oocyte, epithelium, neuron and muscle. *Development* **124**, 461-470.
Debec, A., Detraves, C., Montmory, C., Geraud, G. and Wright, M. (1995). Polar organization of gamma-tubulin in acentriolar mitotic spindles of Drosophila melanogaster cells. *J Cell Sci* **108 (Pt 7)**, 2645-53.
Doerflinger, H., Benton, R., Shulman, J. M. and St Johnston, D. (2003). The role of PAR-1 in regulating the polarised microtubule cytoskeleton in the Drosophila follicular epithelium. *Development* **130**, 3965-75.
Duncan, J. E. and Warrior, R. (2002). The cytoplasmic dynein and kinesin motors have interdependent roles in patterning the Drosophila oocyte. *Curr Biol* **12**, 1982-91.
Ephrussi, A., Dickinson, L. K. and Lehmann, R. (1991). Oskar Organizes the Germ Plasma and Directs Localization Of the Posterior Determinant Nanos. *Cell* **66**, 37-50.
Hollenbeck, P. J. (1989). The distribution, abundance and subcellular localization of kinesin. *J Cell Biol* **108**, 2335-42.
Gonzalez-Reyes, A., Elliott, H. and St Johnston, D. (1995). Polarization of both major body axes in Drosophila by gurken-torpedo signalling. *Nature* **375**, 654-658.
Guichet, A., Peri, F. and Roth, S. (2001). Stable anterior anchoring of the oocyte nucleus is required to establish dorsoventral polarity of the Drosophila egg. *Dev Biol* **237**, 93-106.
Gruss, O. J., Carazo-Salas, R. E., Schatz, C. A., Guarguaglini, G., Kast, J., Wilm, M., Le Bot, N., Vernos, I., Karsenti, E. and Mattaj, I. W. (2001). Ran induces spindle assembly by reversing the inhibitory effect of importin alpha on TPX2 activity. *Cell* **104**, 83-93.
Januschke, J., Gervais, L., Dass, S., Kaltschmidt, J. A., Lopez-Schier, H., Johnston, D. S., Brand, A. H., Roth, S. and Guichet, A. (2002). Polar transport in the Drosophila oocyte requires Dynein and Kinesin I cooperation. *Curr Biol* **12**, 1971-81.
Kawaguchi, S. and Zheng, Y. (2004). Characterization of a Drosophila centrosome protein CP309 that shares homology with Kendrin and CG-NAP. *Mol Biol Cell* **15**, 37-45.
Keryer, G., Di Fiore, B., Celati, C., Lechtreck, K. F., Mogensen, M., Delouvee, A., Lavia, P., Bornens, M. and Tassin, A. M. (2003). Part of Ran is associated with AKAP450 at the centrosome: involvement in microtubule-organizing activity. *Mol Biol Cell* **14**, 4260-71.
Kilmartin, J. V., Wright, B. and Milstein, C. (1982). Rat monoclonal antitubulin antibodies derived by using a new nonsecreting rat cell line. *J Cell Biol* **93**, 576-82.
MacDougall, N., Clark, A., MacDougall, E. and Davis, I. (2003). Drosophila gurken (TGFalpha) mRNA localizes as particles that move within the oocyte in two dynein-dependent steps. *Dev Cell* **4**, 307-19.
Mahowald, A. P. and Strassheim, J. M. (1970). Intercellular migration of centrioles in the germarium of Drosophila melanogaster. An electron microscopic study. *J Cell Biol* **45**, 306-20.

Manseau, L., Calley, J. and Phan, H. (1996). Profilin is required for posterior patterning of the Drosophila oocyte. *Development* **122**, 2109-2116.
Martinez-Campos, M., Basto, R., Baker, J., Kernan, M. and Raff, J. W. (2004). The Drosophila pericentrin-like protein is essential for cilia/flagella function, but appears to be dispensable for mitosis. *J Cell Biol* **165**, 673-83.
Micklem, D. R., Dasgupta, R., Elliott, H., Gergely, F., Davidson, C., Brand, A., Gonzalez-Reyes, A. and St Johnston, D. (1997). The mago nashi gene is required for the polarisation of the oocyte and the formation of perpendicular axes in Drosophila. *Curr Biol* **7**, 468-78.
Montell, D. J., Keshishian, H. and Spradling, A. C. (1991). Laser Ablation Studies Of the Role Of the Drosophila Oocyte Nucleus In Pattern Formation. *Science* **254**, 290-293.
Neuman-Silberberg, F. S. and Schuepbach, T. (1993). The Drosophila dorsoventral patterning gene gurken produces a dorsally localized RNA and encodes a TGF-alpha-like protein. *Cell* **75**, 165-174.
Palacios, I. M. and St Johnston, D. (2001). Getting the message across: the intracellular localization of mRNAs in higher eukaryotes. *Annu Rev Cell Dev Biol* **17**, 569-614.
Palacios, I. M. and St Johnston, D. (2002). Kinesin light chain-independent function of the Kinesin heavy chain in cytoplasmic streaming and posterior localisation in the Drosophila oocyte. *Development* **129**, 5473-85.
Pizon, V., Iakovenko, A., Van Der Ven, P. F., Kelly, R., Fatu, C., Furst, D. O., Karsenti, E. and Gautel, M. (2002). Transient association of titin and myosin with microtubules in nascent myofibrils directed by the MURF2 RING-finger protein. *J Cell Sci* **115**, 4469-82.
Raynaud-Messina, B., Debec, A., Tollon, Y., Gares, M. and Wright, M. (2001). Differential properties of the two Drosophila gamma-tubulin isotypes. *Eur J Cell Biol* **80**, 643-9.
Rebollo, E., Llamazares, S., Reina, J. and Gonzalez, C. (2004). Contribution of noncentrosomal microtubules to spindle assembly in Drosophila spermatocytes. *PLoS Biol* **2**, E8.
Riechmann, V. and Ephrussi, A. (2001). Axis formation during Drosophila oogenesis. *Curr Opin Genet Dev* **11**, 374-83.
Roth, S., Neuman-Silberberg, F. S., Barcelo, G. and Schupbach, T. (1995). Cornichon and the EGF receptor signaling process are necessary for both anterior-posterior and dorsal-ventral pattern formation in Drosophila. *Cell* **81**, 967-978.
Sampaio, P., Rebollo, E., Varmark, H., Sunkel, C. E. and Gonzalez, C. (2001). Organized microtubule arrays in gamma-tubulin-depleted Drosophila spermatocytes. *Curr Biol* **11**, 1788-93.
Schnorrer, F., Luschnig, S., Koch, I. and Nusslein-Volhard, C. (2002). Gamma-tubulin37C and gamma-tubulin ring complex protein 75 are essential for bicoid RNA localization during drosophila oogenesis. *Dev Cell* **3**, 685-96.
Sunkel, C. E., Gomes, R., Sampaio, P., Perdigao, J. and Gonzalez, C. (1995). Gamma-tubulin is required for the structure and function of the microtubule organizing centre in Drosophila neuroblasts. *Embo J* **14**, 28-36.
Tassin, A. M., Maro, B. and Bornens, M. (1985). Fate of microtubule-organizing centers during myogenesis in vitro. *J Cell Biol* **100**, 35-46.
Tavosanis, G. and Gonzalez, C. (2003). gamma-Tubulin function during female germ-cell development and oogenesis in Drosophila. *Proc Natl Acad Sci U S A* **100**, 10263-8.
Theurkauf, W. E. (1994). Premature microtubule-dependent cytoplasmic streaming in cappuccino and spire mutant oocytes. *Science* **265**, 2093-6.
Theurkauf, W. E., Alberts, B. M., Jan, Y. N. and Jongens, T. A. (1993). A central role for microtubules in the differentiation of Drosophila oocytes. *Development* **118**, 1169-80.

Theurkauf, W. E., Smiley, S., Wong, M. L. and Alberts, B. M. (1992). Reorganization of the cytoskeleton during Drosophila oogenesis: implications for axis specification and intercellular transport. *Development* **115**, 923-36.
Walczak, C. E., Mitchison, T. J. and Desai, A. (1996). XKCM1: a Xenopus kinesin-related protein that regulates microtubule dynamics during mitotic spindle assembly. *Cell* **84**, 37-47.
Wilkie, G. S. and Davis, I. (2001). Drosophila wingless and pair-rule transcripts localize apically by dynein-mediated transport of RNA particles. *Cell* **105**, 209-19.

FIGURE LEGENDS

Figure 1. MTOC material and centrioles localizes to the oocyte nucleus during mid-oogenesis. In stage 6 (A) and stage 8 (B), γ Tub37C, (Rb1011, red) is detected around the oocyte nucleus and as a dot close to it (arrowheads A, B). (A-C) DNA green. (C) γTub23C (R77, red) is detected around the oocyte nucleus at stage 8. A similar distribution is observed at stage 6 (data not shown). (D - G) Egg chambers expressing GFP-cter-D-PLP. (D) 3D reconstruction of the oocyte nucleus. D-PLP is detected as a dot (light blue, arrowhead) on the surface of the nucleus (inset, original data). (E-G) D-PLP (single view in E, green) and γTub37C (single view in F, red) colocalize (G) during stage 8 to the same dot close to the nucleus (arrowheads). (H) Polyglutamylated MTs (ID5 antibody) are detected as a dot in the vicinity of the nucleus during stage 9 (arrowhead, inset magnification view). (I, J) Electron micrographs of the anterior dorsal corner of the oocyte, anterior is to the top, dorsal to the right. (I) Low power magnification of the area around the oocyte nucleus. The centrioles are found in the boxed area. (J) At high magnification, two centrioles (white arrowheads) are visible, most likely there are two more (black arrowheads). Golgi cisternae are in the vicinity of the centrioles (arrow). (K) Egg chamber expressing D-PLP. The centrosome is found close to the nucleus (arrow; oocyte outline indicated with dashed line). (L-N) Flies fed with colchicine. (L) The nucleus is misplaced and anti–Khc staining revealed MTs only in the follicle cells. The centrioles (arrows) are separated from the oocyte nucleus in a stage 8 (M) or stage 9 (N) oocyte expressing D-PLP. Asterisk, oocyte nucleus; bar, 20μm (1μm for I and J).

Figure 2. Comparative analysis of MTs in living and fixed egg chambers. MTs in fixed stage 8 egg chambers detected with anti-αTubulin-FITC (A) and anti-Khc (B) (inset in B specificity

of the anti-Khc antibody, a *Khc*$^{7.288}$ mutant germ line clone shows no anti-Khc staining in the oocyte). (C, D, E) stage 7 egg chambers, (F, G, H) stage 9 egg chambers. (C, F) Living egg chambers expressing GFP-αTubulin. (D, G) Fixed egg chambers stained with anti-αTubulin-FITC. (E, H) Fixed egg chambers stained with anti-Khc. (I, J) Stage 9 egg chambers, Khc (red) and aromatic c-ter amino acid of αTub (green). The arrow in J points to the posterior Khc pool.

Figure 3. Extraction procedure is not affecting egg chamber polarity.

(A) Surface view of a fixed stage 10 egg chamber stained for anti-αTubulin-FITC. (B, C) MTs in stretched follicle cells revealed by anti-αTubulin-FITC in fixed egg chamber (B) and by GFP-αTubulin in living eggchamber (C,). MTs in main body follicle cells revealed by anti-αTubulin-FITC in fixed egg chamber (D) and by GFP-αTubulin in living egg chamber (E). (F, G) atypical protein kinase C. Posterior follicle cells fixed after a standard procedure using 4% paraformaldehyde (F) or after the extraction protocol (G). (H, I) Fixed oocyte expressing Kin::LacZ, stained for anti-Khc (red) and anti-β-Gal (green) (Arrow, posterior fraction of Khc). (J, K) Fixed oocyte expressing Nod::LacZ, stained for anti-Khc (red) and anti-β-Gal (green) (Arrows, anterior distribution of Nod). Grk (L) and Osk (M) protein after the extraction protocol. Bar, 20μm.

Figure 4. Two different MT subsets coexist inside the oocyte. Optical planes from confocal Z-sectioning of oocytes stained with anti-Khc according to the sectioning experimental setup presented in (A). 1-5 represent the position of representative optical sections in a WT oocyte (1 represents the most proximal plane close to the cortex and 5, the most distal plane). (B) stage 6, (C) stage 7, (D) stage 8 and (E) stage 9 oocytes. Two MT subsets can be

distinguished according to orientation and stage-dependent changes. The DV subset: throughout oogenesis, cortical MTs oriented along the DV axis could be observed. At the proximal and distal cortices MTs running parallel to the DV axis can be seen from stage 7 on (C 1, 5; D 1, 5; E 1, 5; white arrowheads) and to a lesser extent in stage 6 (B 1, 5; white arrowheads). The AP subset: (B) Before oocyte re-polarization at stage 6, MTs extend along the cortex and fold back slightly at the anterior (B, 2 and 3, red arrowheads). The nucleus is encapsulated by MTs and short fibers point from the nucleus toward the anterior (B, 3 and 4, arrows). (C) By stage 7, long MTs are rolled up in the shape of a "diaphragm" in the centre of the oocyte (C, 2-4). MT bundles emanate from the perinuclear region project toward the cortex (C 2, arrow). The centre of the cytoplasm contains only few MT fibers. (D) In stage 8, the "diaphragm" has opened and MT bundles project from the anterior in AP direction (D 2, arrow). MTs bundle at the posterior and join the centre (D 3, arrow). Transversal sections of MTs appear as dots on the ventral side of the oocyte (D 3 arrowhead). Free MT ends are found in the centre of the oocyte (D 4, arrowheads). (E) In stage 9, the central MTs originate from the anterior and the oocyte nucleus (E, 2 and 3, arrows). One or two thick bundles that resemble a "horse shoe" like pattern orient in AP direction (E 4, arrows). (B 6, C 6, D 6, E 6) Schematic representations of the MT distribution at mid-oogenesis. (B 6) MT distribution before re-polarization is shown in blue. After re-polarization, the invariant DV subset is depicted in black, the dynamic AP subset in red. (C 6) Stage 7 (*diaphragm* state). (D 6) Stage 8 (*open diaphragm* state). (E 6) Stage 9 (*horse shoe* state). (F-H) Living egg chambers expressing Tau-GFP. (F) The cortical DV (arrowhead) subset can be detected in living stage 8 oocyte. (G) Stage 10A oocyte where two MT bundles in AP orientation can be seen in the centre (arrows). (H) Stage 11: thin bundles of MTs can be detected in DV orientation (arrowhead) close to the cortex. Red dotted lines mark the outline of the oocyte. Asterisk, location of oocyte nucleus, bar 20µm.

Figure 5. The nucleus is an active centre for MT polymerization. (A) Schematic representation of the experimental setup for cold-induced MT disassembly. Complete de-polymerization: dissected ovaries were extracted (30min), placed on ice (30min), fixed and analyzed for MTs by anti-Khc. To allow MT regrowth, ovaries were incubated at 25°C for 3 to 30min. (B) Stage 9 oocyte, complete MT de-polymerization. Khc was only detectable at the posterior (arrowhead). (C) Cold-shock treatment did not alter γTub37C localization (arrowhead). (D, E) Centres of MT polymerization (arrowhead) were detected in the vicinity of the oocyte nucleus, never at the posterior or at cortical regions after short recovery times. (F) MTs appears along the anterior margin after 10 min regrowth. (G) MT regrowth along the cortex in DV orientation during intermediate recovery times. (H) Optical section taken in the centre of the same oocyte as in G. Clouds of Khc positives dots at the ventral and dorsal sides (arrowheads) represented transverse cuts of the cortical MTs. The AP subset in the centre was not yet established. (I, J) Optical section of the same oocyte. 30min recovery at 25°C was sufficient to regrowth MTs to the control situation. Cortical DV subset (I arrowhead) and, in the centre (J), MTs in AP direction (arrow) Asterisk, oocyte nucleus, bar 20µm.

Figure 6. *grk* mutant oocytes conserve the MT configuration of wild-type stage 6 oocytes. (A-B) *grk* mutant egg chambers stained for anti-Khc. In oocytes comparable to WT stage 8 (A) and stage 9 (B), the nucleus is misplaced to the posterior and surrounded by MTs. (C) Schematic representation of the MT network in *grk* oocytes. (D) *grk* stage 9 oocyte showing the accumulation of Khc (arrow) between the MT extremities of the long cortical MTs (red

arrowheads) and the short central MTs (white arrowhead). (E, F) WT stage 6 oocytes showing a similar MT distribution. MT bundles project from the nucleus at the posterior along the cortex to the anterior where they bend back to the centre (red arrowheads). Short bundles stretch out from the nucleus into the centre of the oocyte (white arrowhead). To better visualize MTs a projection of 10 optical sections (4µm) is shown in (F). (G) Egg chamber expressing Kinesin:βGal (green) costained for Khc (red). (H) γTub37C (R46) localizes to the nucleus at the posterior in *grk* mutant oocytes and the centrosome close to it (arrow). (I) *grk* mutant oocyte showing complete de-polymerization of MTs after 30 min cold-shock. (J) *grk* mutant oocyte (projection of 5µm) after a 15min recovery at 25°C. MTs regrow from the misplaced nucleus at the posterior. Asterisk, oocyte nucleus. Bar, 20µm.

Figure 7. Correlation of the stage-dependent MT organization and *grk* as well as *osk* mRNA localization from stage 7 through stage 9. *grk* (green) and *osk* (blue) are visualized by fluorescent in situ hybridization. At stage 7, *grk* and *osk* are found mostly at the anterior cortex. *grk* is rapidly transported toward the oocyte nucleus in the transition from stage 7 to stage 8, exploiting the DV MT subset (black). The DV subset comprises long cortical MT fibres as well as the shorter cortical fibres. *osk* mRNA localization correlates with the successive progression of AP MT subset (red) formation. *osk* is transported from the anterior toward the centre following the open diaphragm MTs in the centre. By stage 9 upon oocyte growth and complete AP orientation of centre MTs, *osk* is transported toward the posterior.

Figure Sup MOV 1. : Animated stack of a complete series of optical sections through a stage 8 oocyte**.** The red arrow tracks MT fibers from the central AP subset back to anterior cortex and the nucleus. The green arrow tracks MT fibers from the cortical DV MT subset back to the oocyte nucleus (nuc). The white arrow follows DV MT bundles from the proximal to the distal cortex demonstrating that MT bundles run cortically. The open circle highlights MT extremities (plus ends) in the center, since once they appear they can be followed only in one direction. Optical sections every ~ 0.2 µm. Note that a certain portion of the cortical fibres does not seem to be connected to the oocyte nucleus. Thus, the DV subset is comprised of long fibres connetced to the oocyte nucleus as well as shorter cortical fibres, extending from the cortex towards the centre of the oocyte.

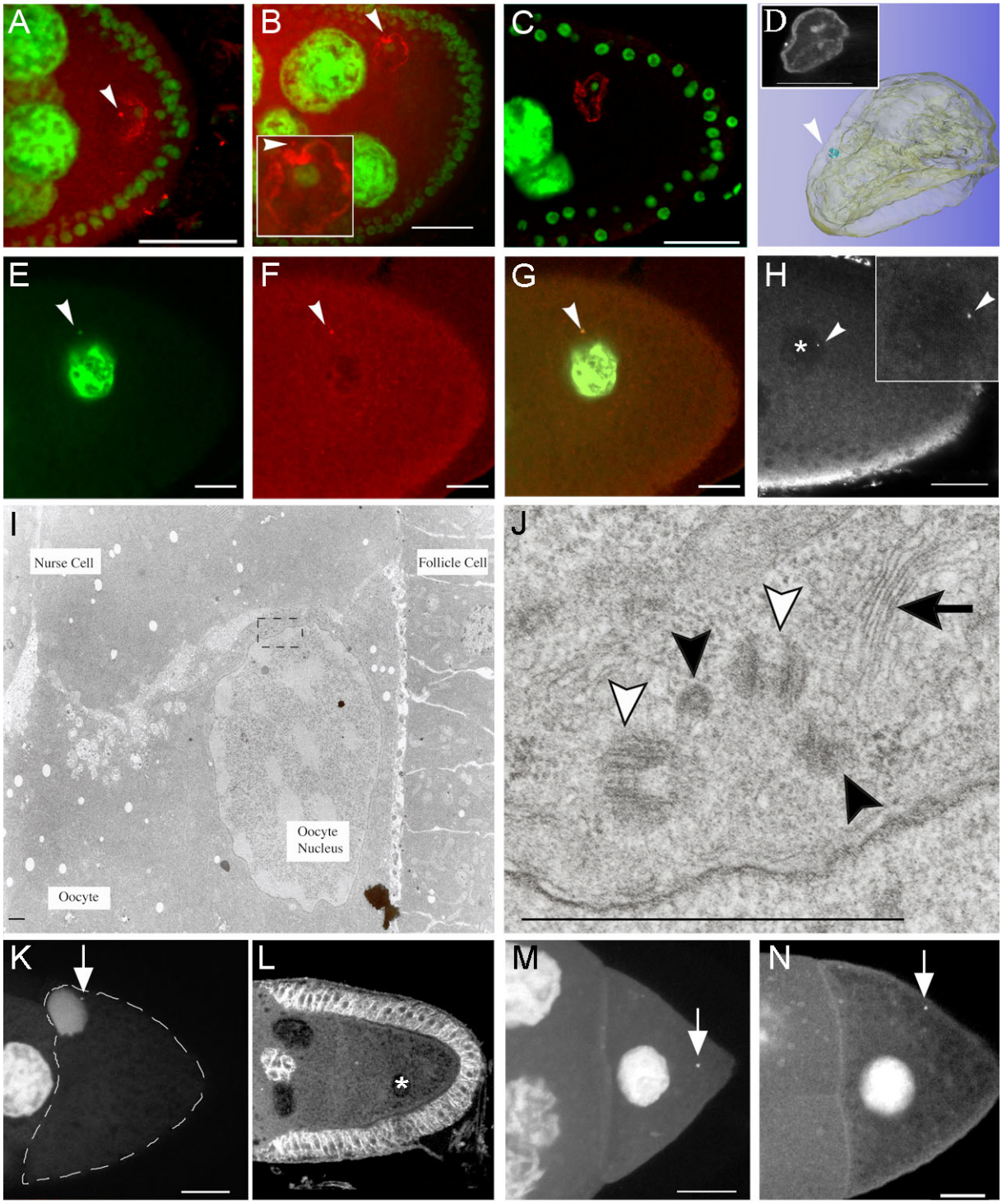

Januschke et al. Fig. 1

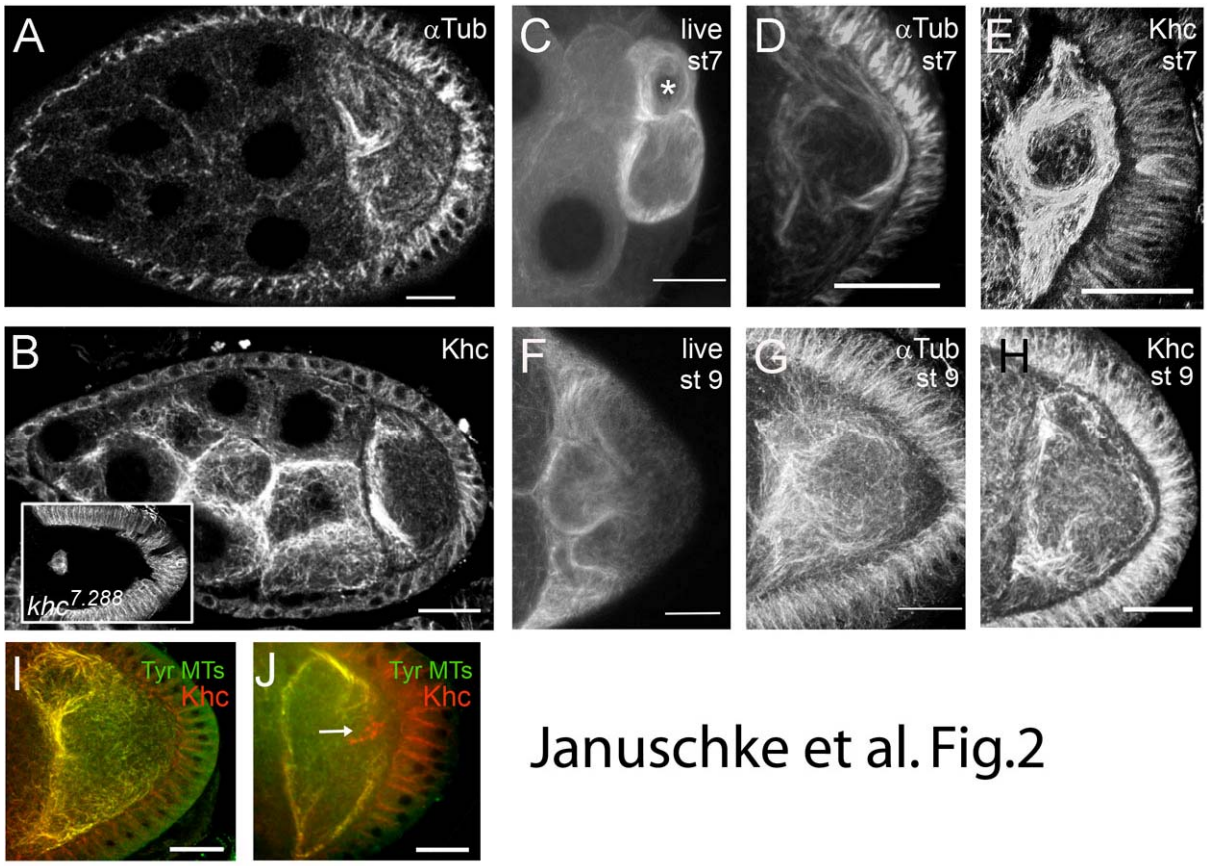

Januschke et al. Fig.2

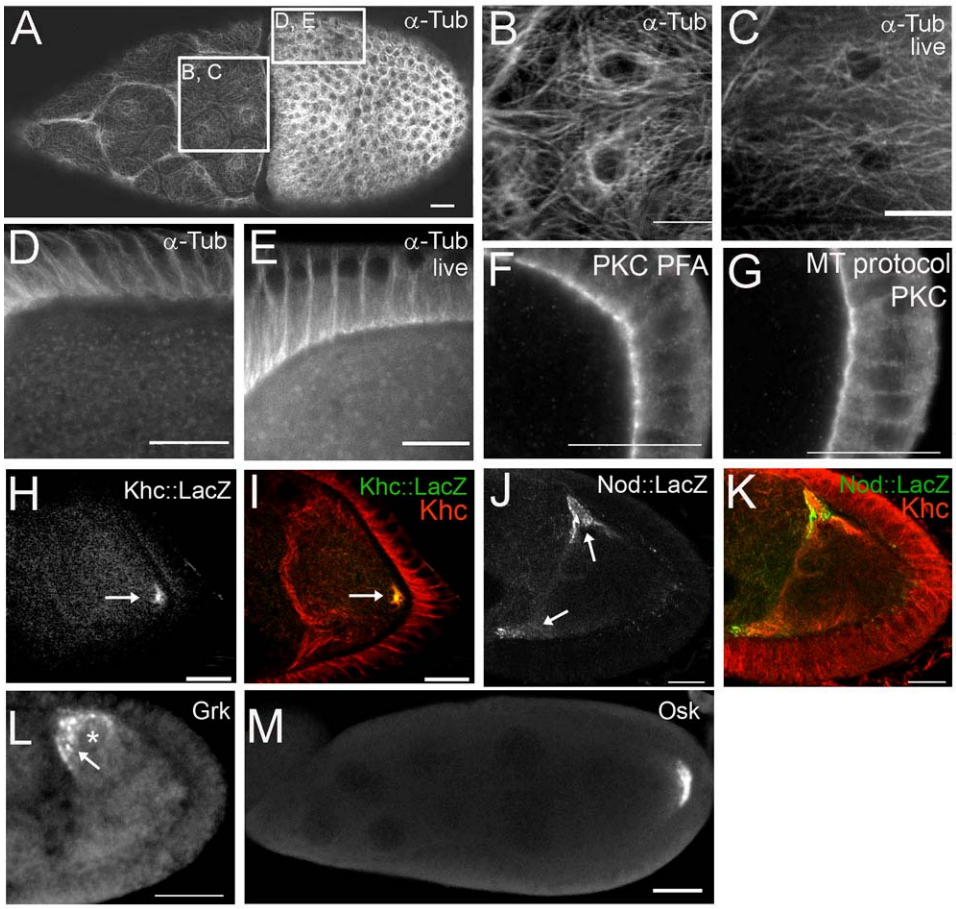

Januschke et al. Fig. 3

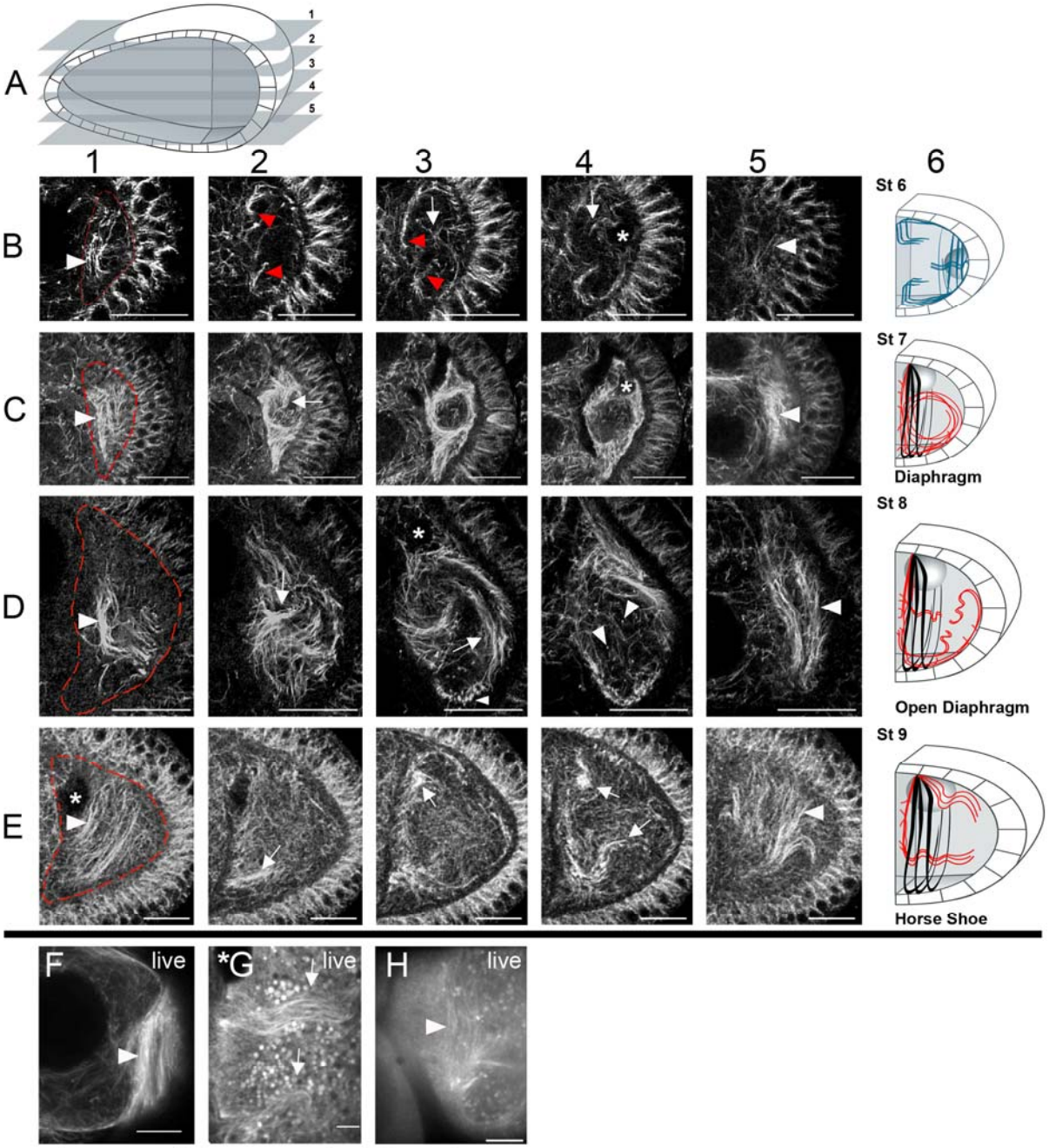

Januschke et al. Fig. 4

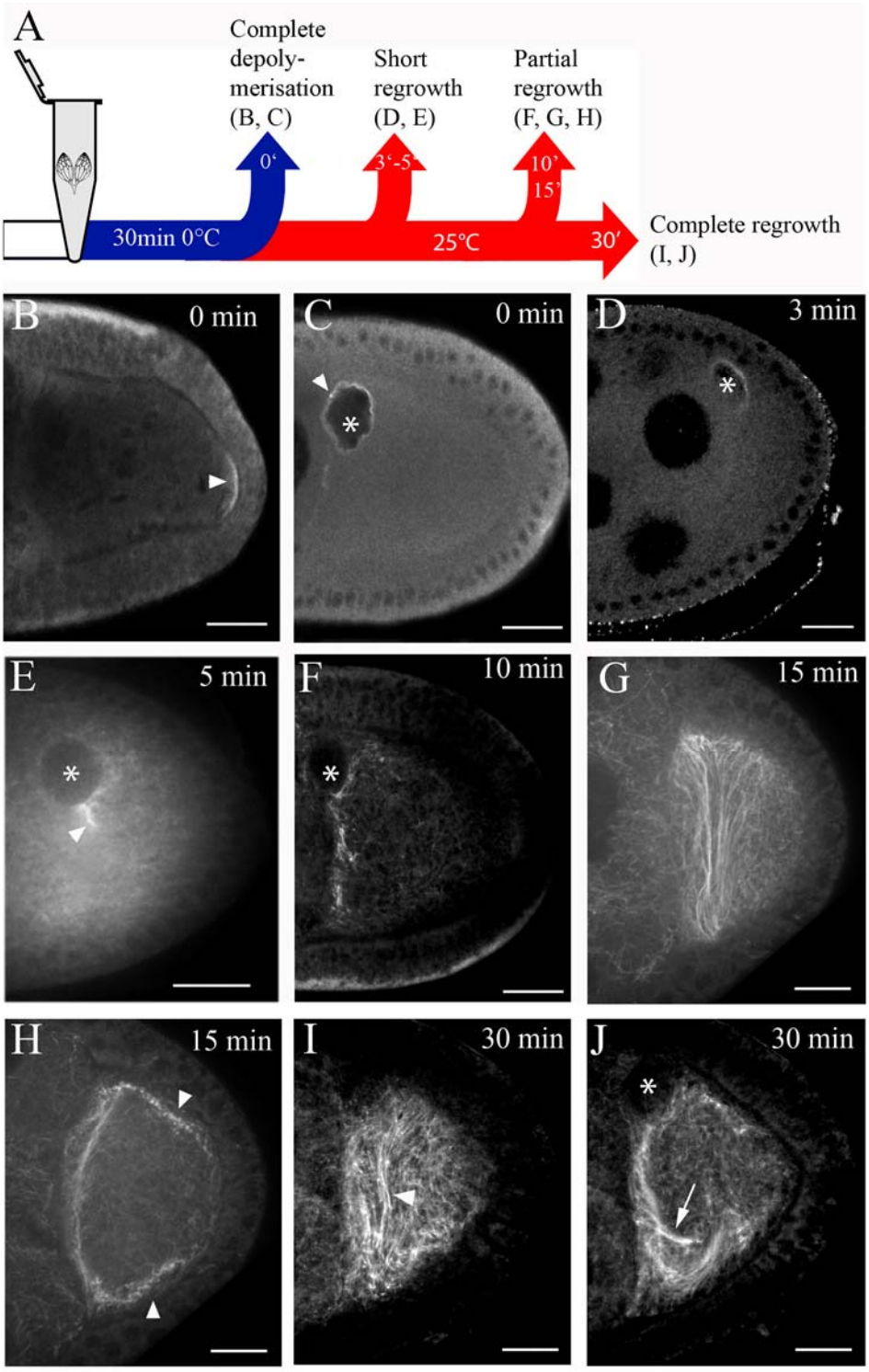

Januschke et al. Fig. 5

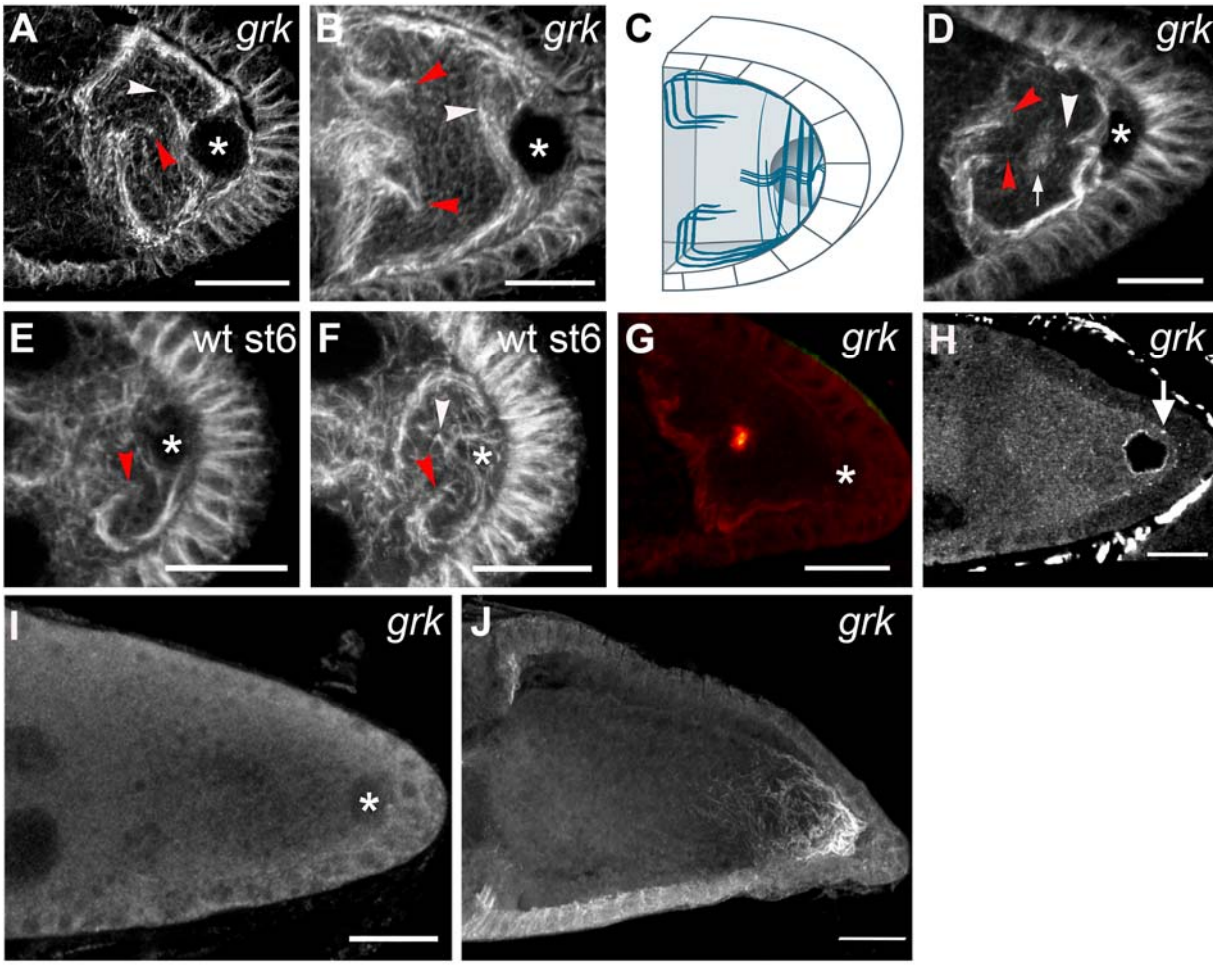

Januschke et al. Fig. 6

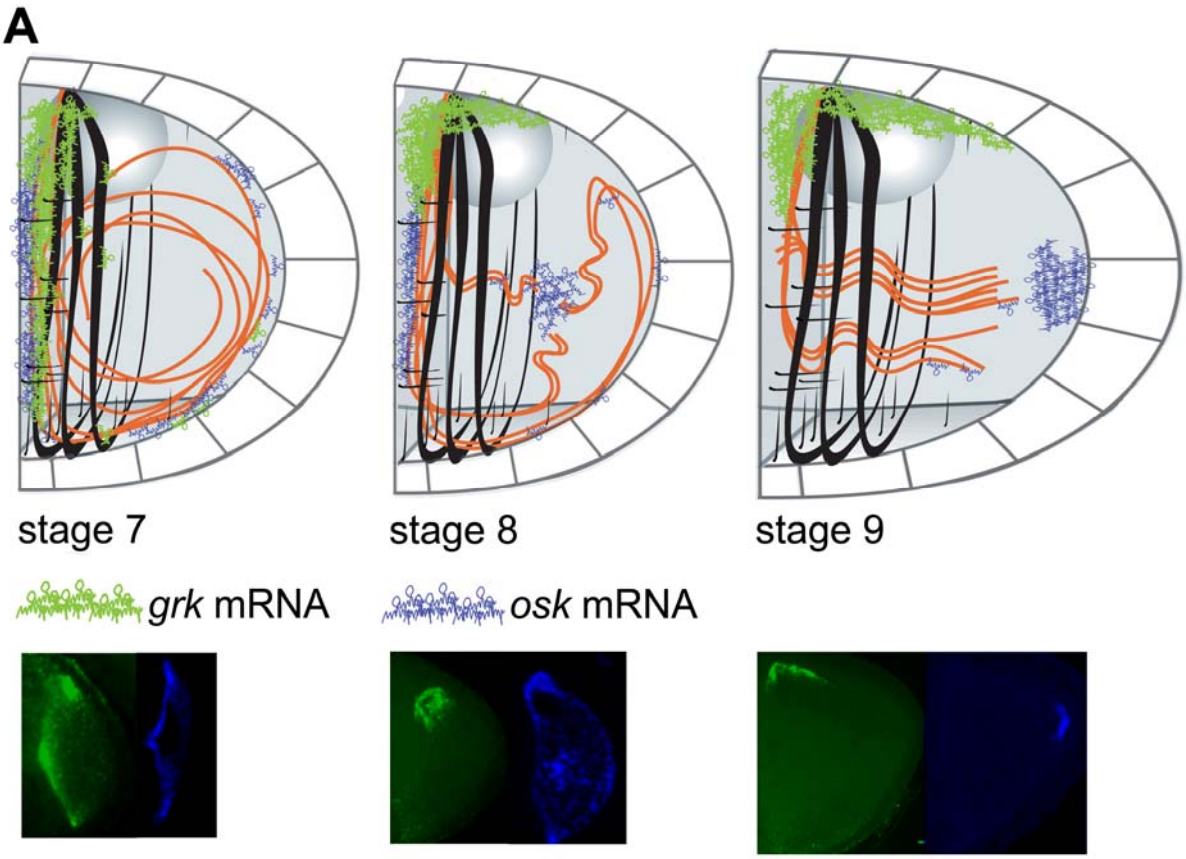

Januschke et al. Fig. 7